On the Prediction of Two-Dimensional Supersonic Viscous Interactions Near Walls

R. I. Issa* and F. C. Lockwood†
Imperial College of Science and Technology, London, United Kingdom

An existing iterative finite-difference prediction method for the solution of the elliptic differential equations governing incompressible flowfields is adapted to handle compressible fields in which both subsonic and supersonic regimes may be present. The basic procedure and its adaptation are described. The modified method is tested against known analytic solutions for some inviscid supersonic flows, and against experimental data for some laminar, and one turbulent, boundary-layer/wave interactions near walls. The method performs tolerably well. The inaccuracies may be attributed to the wave smearing consequent of the finite-difference treatment.

Nomenclature

h = stagnation enthalpy
M = Mach number
p = pressure
$\dot{q}$ = heat-transfer rate
R = gas constant
Re = Reynolds number
S = volumetric source rate
St = Stanton number
T = static temperature
T_w = wall temperature
u = x-directed velocity
v = y-directed velocity
x = streamwise coordinate
$\tilde{x}$ = x divided by length of integration domain
y = cross stream coordinate
α = angle of incidence of shock
γ = ratio of specific heats
δ = displacement thickness
Γ = diffusion transport coefficient
μ = fluid viscosity
ρ = density
σ = Prandtl number
ϕ = a dependent variable.

I. Introduction

A. The Problem Considered

THE presence of a wall in supersonic flow gives rise to a complex 'supersonic viscous interaction' between the subsonic layer very near the wall and the adjacent supersonic region. The interaction arises because influences of the pressure waves embedded in the supersonic region propagate upstream through the subsonic layer. The streamline directions in the subsonic layer alter to accommodate these pressure effects. The neighboring streamlines in the supersonic region are correspondingly altered, but because the supersonic pressure field is very sensitive to streamline angle, it is significantly affected by relatively small adjustments in the subsonic layer. The wall-bounded supersonic flow is, therefore, not 'hyperbolic/parabolic' in kind, rather it possesses a mixture of 'hyperbolic' and 'elliptic' features.

The interaction between the shock wave, which springs from the entrance lip of the engine-intake duct of a supersonic aircraft, and the duct wall boundary layer is an important engineering flow which falls into the present class. The elliptic influence of the subsonic layer is manifest in the thickening of the boundary layer which occurs, in response to the pressure rise of the shock, in advance of the shock impingement location. If the shock is moderately strong, the boundary layer separates, and a region of recirculation forms about the impingement location. The consequent wave system in the supersonic field is very markedly different from that corresponding to inviscid flow analysis.

Some recent computational studies by the present authors[1] have demonstrated that the supersonic/viscous interaction may exert an overriding influence on the flow structure even when its strength is not sufficient to induce separation. Account of the interaction must be taken in any prediction method which purports the ability to handle virtually any of the whole range of flows associated with transonic, as well as supersonic, flight regimes. This paper is concerned with such a prediction procedure.

B. Previous Work

Several integral-profile approaches to the prediction of the interaction between a shock wave and a boundary layer mentioned in the preceding section appear in early and recent literature (see Refs. 2 to 7, for example). The most well known of these is probably that due to Lees and Reeves.[6] In spite of their extreme simplicity, it is fair to say that these methods have resulted in surprisingly good predictions of some of the more general features of the flow, for the narrow range of conditions for which they were intended.

The emergence of finite-difference methods has provided a means of obtaining detailed predictions for many generalized flow situations; however, this potential is far from realized at the present time. Many calculations of supersonic boundary layers have been performed using finite-difference techniques of the 'parabolic' variety (see Refs. 8 to 12, for example), but these methods are unable to handle the elliptic features of the supersonic/viscous interaction. Some of these methods have attempted to take account of the interaction within the sphere of the parabolic prediction method, but the computations have invariably exhibited instabilities which cannot be suppressed in any universal and satisfactory way. Indeed, Garvine[13] has shown that the instabilities are the inevitable result of the use of a parabolic procedure to predict what is properly an elliptic flow.

Methods which account for elliptic effects in supersonic viscous interactions have been developed and used to good effect; see, for example, Refs. 14 to 18. These methods are capable of solving the Navier-Stokes equations which embody

Received Feb. 9, 1976; revision received Sept. 24, 1976.
Index categories: Shock Waves and Detonations; Subsonic and Transonic Flow; Supersonic and Hypersonic Flow.
*Consultant Engineer.
†Lecturer, Mechanical Engineering Dept.

all the physical features of fluid flow in general. The above-mentioned methods use the time-dependent form of the governing equations which yield the desired steady-state solution when their integration is carried over a long period of time. The advantage of this approach is that the time-dependent equations are of hyperbolic/parabolic nature and can be solved by a marching integration scheme and, in consequence, the numerical solution procedure becomes particularly simple.

Solutions by these methods have been obtained for hypersonic-viscous interactions occurring at the leading edges of flat plates,[14-17] while Goodrich et al.[14] have also computed the flow past a backward facing step and the near wake of a blunt trailing edge. Good agreement between these calculations and experimental data is generally reported. Baldwin and MacCormack[18] have computed a range of shock wave/boundary-layer interaction problems with success; their method appears to be reasonably efficient.

Another method which attempts to account for some of the elliptic effects in supersonic viscous interactions is that due to Werle and Vatsa.[19] They employ a boundary-layer approach with alternating direction of integration.

The disadvantages of the time-marching techniques are that they are prone to numerical instability and are slow to converge to the final steady-state solution. The solution of the steady-state form of the Navier-Stokes equations, on the other hand, does not suffer from the same limitations of the time-marching method. However, it has not been possible until recently to achieve a simple coupling of the solution of the momentum equations with the solution of the continuity equation. Recently, a general computational procedure for two- and three-dimensional flows has been developed which employs directly the 'primitive' variables, i.e., pressure and the two/three velocity components.[20,21] There has so far been no reported application of this method to compressible flows.

C. Purpose and Scope of the Present Contribution

The present paper is concerned with the modification and development of the pressure-velocity method[20,21] for the prediction of the supersonic/viscous interaction and the subsequent validation of the modified method for two-dimensional flow situations. The equations to be solved are given in Sec. IIA while the basic method is briefly reviewed in Sec. IIB. The modifications which have been incorporated in the adaptation of the basic method to supersonic flow are described in Sec. IIC. Sec. III is concerned with the validation work; solutions for an inviscid flow are obtained in Sec. IIIA; and in IIIB the method is tested against experimental data for three near-wall viscous flows. Some conclusions are drawn in Sec. IV.

II. Governing Equations and Method of Solution

A. The Governing Equations

The independent variables of the problem are the axial (x) and lateral (y) coordinates of a Cartesian system; the x-coordinate is aligned in the predominant direction of flow. The main dependent variables solved are: u) the axial velocity component, v) the lateral velocity component, p) the static pressure, and h) the stagnation enthalpy.

The method solves transport equations possessing the form

$$\frac{\partial}{\partial x}(\rho u\phi)+\frac{\partial}{\partial y}(\rho v\phi)=\frac{\partial}{\partial x}\left(\Gamma_\phi\frac{\partial\phi}{\partial x}\right)+\frac{\partial}{\partial y}\left(\Gamma_\phi\frac{\partial\phi}{\partial y}\right)+S_\phi \tag{1}$$

where: a) ϕ may stand for u, v, or h; b) Γ_ϕ is the local effective exchange coefficient for the variable ϕ. It is given by: $\Gamma_u\equiv\mu$ (the fluid viscosity which may be assigned effective values when the flow is turbulent); $\Gamma_v\equiv\mu$, $\Gamma_h\equiv\mu/\sigma$, where σ is the Prandtl number. c) S_ϕ is the source (or sink) of the variable ϕ. It assumes different forms when ϕ stands for the different variables; the forms used in the present work are given by:

$$S_u\equiv\frac{\partial}{\partial x}\left(\mu\frac{\partial u}{\partial x}\right)+\frac{\partial}{\partial y}\left(\mu\frac{\partial v}{\partial x}\right)-\frac{\partial p}{\partial x}\qquad M<1 \tag{2a}$$

$$S_u\equiv-\frac{\partial p}{\partial x}\qquad M>1 \tag{2b}$$

$$S_v\equiv\frac{\partial}{\partial x}\left(\mu\frac{\partial u}{\partial y}\right)+\frac{\partial}{\partial y}\left(\mu\frac{\partial v}{\partial y}\right)-\frac{\partial p}{\partial y}\qquad M<1 \tag{3a}$$

$$S_v\equiv-\frac{\partial p}{\partial y}\qquad M>1 \tag{3b}$$

$$S_h\equiv\frac{\partial}{\partial x}\left[\mu\left(1-\frac{1}{\sigma}\right)\frac{\partial}{\partial x}\left(\frac{u^2+v^2}{2}\right)\right]+\frac{\partial}{\partial y}\left[\mu\left(1-\frac{1}{\sigma}\right)\frac{\partial}{\partial y}\left(\frac{u^2+v^2}{2}\right)\right]\qquad M<1 \tag{4a}$$

$$S_h\equiv\frac{\partial}{\partial y}\left[\mu\left(1-\frac{1}{\sigma}\right)\frac{\partial}{\partial y}\left(\frac{u^2+v^2}{2}\right)\right]\qquad M>1 \tag{4b}$$

For the flows examined here, the diffusion in the x-direction was neglected in the supersonic region, and the relevant terms in Eqs. (2) to (4) are omitted for $M>1$. The velocity-divergence terms

$$\frac{\partial}{\partial x}\left[-\frac{2}{3}\mu\left(\frac{\partial u}{\partial x}+\frac{\partial v}{\partial y}\right)\right]$$

and

$$\frac{\partial}{\partial y}\left[-\frac{2}{3}\mu\left(\frac{\partial u}{\partial x}+\frac{\partial v}{\partial y}\right)\right]$$

which have been omitted from Eqs. (2) and (3) are also insignificant in all regions where the x-direction diffusion effects are small. Where such diffusion effects become large, namely in regions of low velocities near the wall, the flow is incompressible, and the terms vanish. They are, therefore, omitted for the sake of economy of computation.

Auxiliary equations that are used are the relationship between the stagnation enthalpy and the static temperature given by

$$h=C_pT+\tfrac{1}{2}(u^2+v^2) \tag{5}$$

where C_p is the constant pressure specific heat and T is the temperature, and the equation of state given by

$$\rho=p/RT \tag{6}$$

where ρ is the static density, and R is the Gas Constant.

The continuity equation closes the set of governing equations; it is given by

$$\frac{\partial}{\partial x}(\rho u)+\frac{\partial}{\partial y}(\rho v)=0 \tag{7}$$

B. The Basic Solution Procedure

The basic solution method is described in detail in Refs. 20 and 21, which give all the expressions arising in the finite-difference formulation, so that only an outline of it is required here. This is provided by the Sec. IIB. Sec. IIC describes the modifications made to the procedure for the handling of compressible flow.

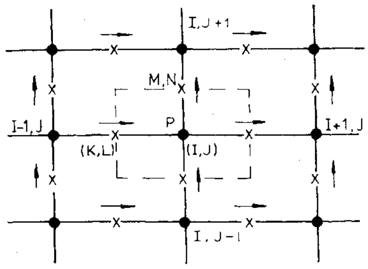

Fig. 1 A typical portion of the finite difference grid.

The basic procedure is of the iterative, finite-difference variety. One of the main features of the method is the use of staggered arrangement of the grid (shown in Fig. 1) to descretize the domain of solution. The velocities are calculated at the locations indicated by the crosses (K,L for example) lying midway between the main grid nodes which are indicated by the dots (I,J for example). The pressure and stagnation enthalpy are stored at the main grid nodes; the u's are located as positions marked by the symbol →, and the v's at those marked by the symbol ↑.

The finite-difference form of Eq. (1) is obtained by integration over a control volume surrounding the node under consideration. A typical control volume surrounding node (I,J) is shown in Fig. 1.‡ This yields an expression of the form

$$\phi_P = \Sigma_n C_n \phi_n + \bar{S}_\phi \tag{8}$$

where P is the central node (which, for example, stands for node (I,J) when $\phi \equiv h$, and for node (K,L) when $\phi \equiv u$); Σ_n represents the summation over the four neighboring points: $(I+1,J)$, $(I,J+1)$, $(I-1,J)$ and $(I,J-1)$,§ and C_n are coefficients expressing the effects of convection and diffusion. A hybrid upwind/central differencing scheme is used in deriving the expressions for C_n. The scheme gives first-to-second-order accuracy depending on the control-volume Reynolds number [see Refs. 20, 22, and 23]. The term $\bar{S}_\phi$ represents the integrated form of the source term $\bar{S}_\phi$. When $\phi \equiv u$ or $\phi \equiv v$, it also contains the pressure gradient terms, [for $u(K,L)$ for example, this will be $(p_{I-1,J} - p_{I,J})$]. There is an equation like (8) for each node, and therefore one set of equations for each of the three dependent variables.

The finite-difference form of the continuity equation (7) is obtained by integration over a control volume surrounding a main grid node [(I,J) for example]. The resulting equation is then used to derive a pressure-correction equation which possesses the same form as Eq. (8). The derivation of the pressure-correction equation proceeds as follows. The u's, v's, and p's in the finite-difference continuity equation are assumed to be perturbed by a change in pressure. Expressions giving the u, v, and p perturbations in terms of the pressure perturbation are then derived from the finite-difference form of the momentum equations and the equation of state. These expressions are combined with the finite-difference continuity equation to eliminate the perturbation terms for u, v, and p and to yield the pressure-correction equation which contains only the pressure perturbation as a dependent variable.

The set of equations (8) are solved over the whole flowfield for one dependent variable at a time. The solution proceeds line by line, and an efficient tri-diagonal matrix algorithm is used for this purpose.

The numerical solution of the sets of equations proceeds as follows:

1) Values of the field variables are guessed. These values are usually taken to be the ones obtained from the previous iteration.

2) The two momentum equations are solved to give new u's and v's.

3) The u's and v's will not satisfy the continuity equations unless the pressure field has been initially guessed correctly. The error in continuity is here calculated at each main grid node.

4) The pressure-correction equation whose purpose is to yield suitable adjustments to the pressure field that will remove the continuity errors is then solved.

5) The u and v-velocities are then adjusted accordingly. The expressions linking the u and v perturbations to the pressure perturbations which were used in the derivation of the pressure-correction equation are employed for the velocity adjustments.

6) The h-equation is solved.

7) The temperature is calculated from the stagnation enthalpy. The density is then calculated from the new pressure and temperatures.

8) A new iteration is started if the solution is not converged.

C. Modifications for Supersonic Flow

The basic method treats the whole flowfield as an elliptic domain whereas there exist, for a supersonic flow, definable 'zones of influence' of a hyperbolic character. There are three sources of 'ellipticity' in the unmodified procedure: a) The variables at every point in the field are linked to their downstream neighbors by the difference equation (8); b) the pressure difference driving the velocity at a velocity node [$u(K,L)$, for example] is that between the two main grid nodes lying either side of the velocity location [$(p_{I-1,J} - p_{I,J})$ for $u(K,L)$]; this implies that downstream pressures influence upstream velocities; c) the calculation of the mass fluxes at the continuity (main) control-volume boundaries is based on linearly interpolated values of densities between the grid nodes. This implies that downstream densities, and hence pressures, affect upstream velocities.

The first of these elliptic numerical influences is effectively eliminated by the hybrid differencing scheme which ignores diffusional effects when the control-volume Reynolds number is large and employs upwind differencing of the convective terms. The second is handled by modifying the u-velocity difference equation such that the pressure difference driving a u-velocity, when the latter is supersonic, is simply taken to be that across the adjacent two upstream nodes. So, for example $\partial p/\partial x$ for $u_{K,L}$ (Fig. 1) is represented by $(p_{I-2,J} - p_{I-1,J})/\delta x$. This in effect means the use of backward differencing for the pressure gradient. The third elliptic influence is removed by the sole use of upstream densities when computing supersonic mass fluxes. So, for example, the mass flux associated with $u_{K,L}$ is expressed as $\rho_{I-1,J} u_{K,L}$.

D. Remarks about the Modified Procedure

Some useful comments about the numerical simulation of a supersonic flow can be made with reference to the sketches in Fig. 2. Panel a) refers to the unmodified procedure and shows a typical grid node (I,J) linked to its immediate four neighbors; whereas in reality the location (I,J) should only be affected by influences transmitted along the characteristic curves. Panel b) shows the ideal numerical linkage, but since the characteristic angles vary throughout the flow and are not known in advance, the required grid cannot be constructed conveniently.

Panel c) shows the linkages between (I,J) and its neighbors achieved by the present modified treatment; clearly it does not simulate entirely the ideal situation shown in panel b). An ostensibly more appealing interlinkage is achieved by an explicit, marching integration scheme characterized by panel d) (such a scheme was used by Ref. 24, among others). However, explicit scheme characterized by panel schemes suffer severe stability limitations compared with the present implicit method.

‡Because of the staggered grid arrangement, the control volumes for the u and v nodes are also staggered relative to the main control volumes.

§Or $(K+1,L)$, $(K,L+1)$, $(K-1,L)$, and $(K,L-1)$ when ϕ stands for u.

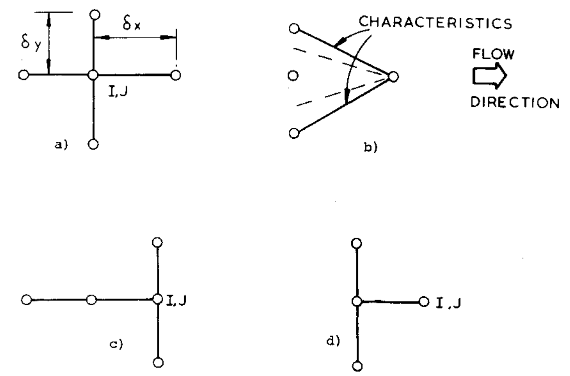

Fig. 2 Some possible interlinkages between grid points.

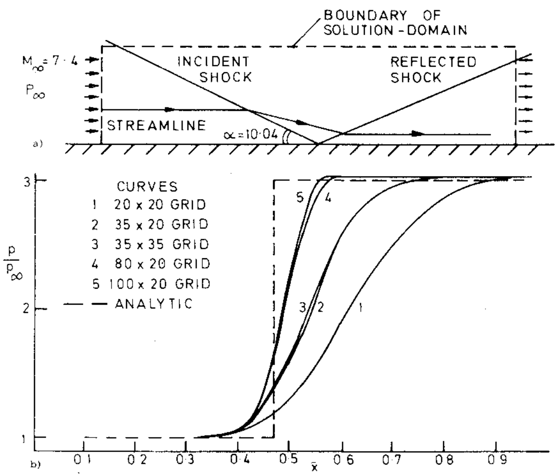

Fig. 3 Inviscid shock reflection: a) flow geometry; b) wall pressure distribution, $M_\infty = 7.4$.

E. Boundary Conditions

Two boundary treatments only require special mention here: 1) that applicable at the outer freestream boundary; and 2) that pertaining at the outflow boundary location. Considering the former, if a wave originates from within the domain of computation, its strength and location at the free boundary are not known in advance. Suppose the location (M,N) in Fig. 1 coincides with a free boundary, we determined the y-directed v-velocity there from the 'simple wave' relation¶

$$V = V_\infty + \left(\frac{\sqrt{M^2-1}}{\gamma M^2}\right) u \ln \frac{p}{p_\infty} \tag{9}$$

The subscript ∞ refers to the freestream condition, and u and M are the mean of the calculated values at the J grid line and the freestream values. When an inward-travelling wave impinged on the freestream boundary, the appropriate v-velocity prevailing just behind the wave was prescribed at the point of impingement.

The outflow boundaries were always located well downstream of the interaction region where the flow is expected to be of a parabolic/hyperbolic nature. The imposition of an outflow constraint in the supersonic zone is of course superfluous. Since the downstream flow was of the boundary-layer kind, we adopted for the subsonic zone the simple expedient of neglecting the x-direction diffusion. Also, the gradient $\partial(\rho u)/\partial x$ was taken as zero. This ensured that all the mass flow entering the last column of control volumes is fluxed out at the outflow boundary. To ensure that this

¶For the definition of simple-wave see Ref. 25.

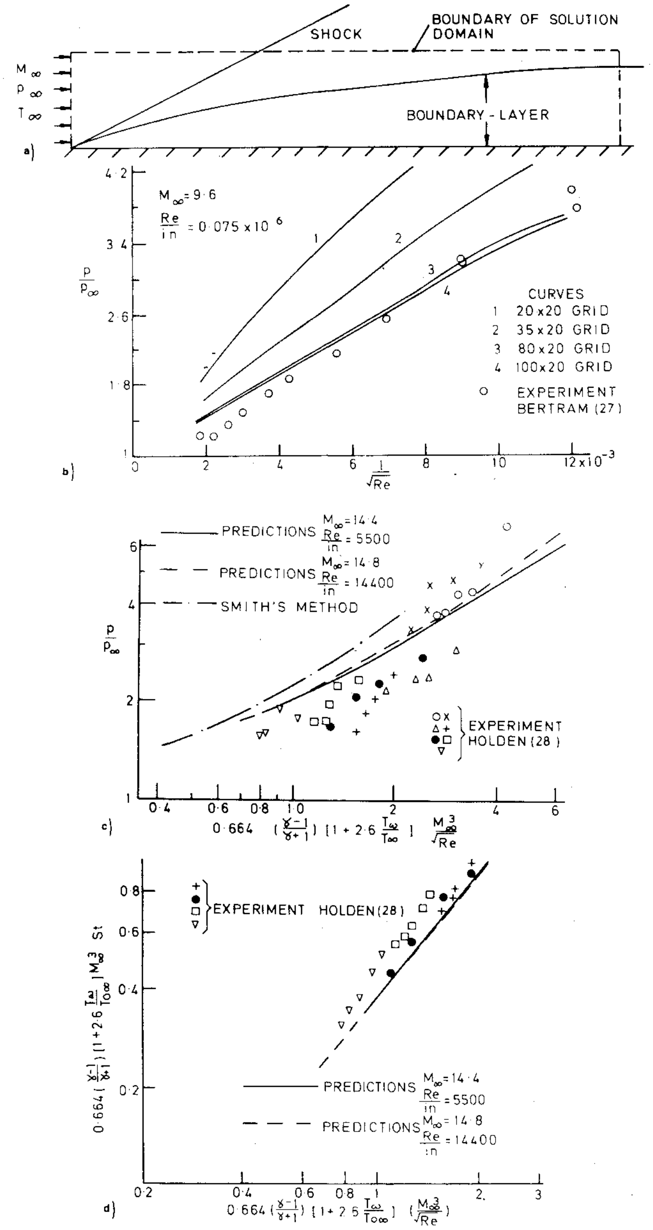

Fig. 4 Laminar hypersonic flow near the sharp leading edge of a flat plate: a) flow geometry; b) wall pressure distribution for experiment of Ref. 27; c) wall pressure distribution; d) wall heat-transfer distribution for experiment of Ref. 28.

constaint did not introduce significant errors, computations with different locations of the outflow boundary were performed.

III. Validation of the Procedure

A. Inviscid Flows

For the purpose of testing the accuracy of the finite-difference scheme, predictions have been made of three supersonic inviscid flows having analytical solutions; they were: the flow over a flat plate inclined to the mainstream direction, the merging of two inviscid streams of differing Mach numbers and pressures, and the reflection of a shock at a wall. Representative results for only the last of these will be reported here a fuller discussion may be found in Ref. 26.

Figure 3 shows the prediction, in the vicinity of the shock impingement location, of the wall pressure distribution for five grid meshes compared with the analytic variation. The results show that the refinement of ∂x considerably improves the resolution of the shock wave. The results also show that when δx is coarse, the refinement of δy does not necessarily

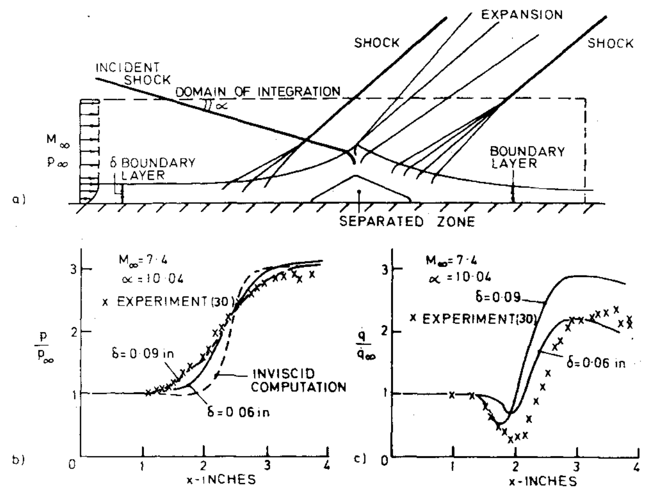

Fig. 5 Laminar flow shock reflection: a) flow geometry; b) wall pressure; c) heat-transfer distributions.

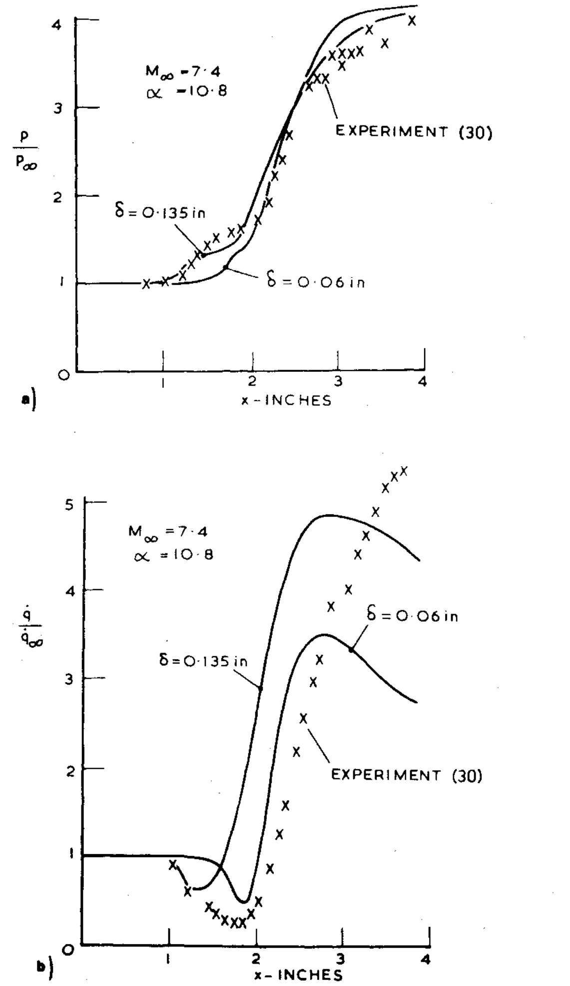

Fig. 6 Laminar flow shock reflection: a) wall pressure; b) heat-transfer distributions.

affect the solution. It is evident that the resolution of the shock is controlled not only by the number of grid nodes in both directions, but also by the ratio $\delta y/\delta x$.

It was apparent from the tests performed, not all of which are shown here, that there is usually an optimum value of $\delta y/\delta x$ below which the refinement of δy does not improve the results. This phenomenon can be explained (with reference to Fig. 2) by the fact that if $\delta x \gg \delta y$, then the zone of influence for every grid node becomes larger than δy. This implies that the grid node is now influenced by its lateral neighbors much more than by the one immediately upstream of it, hence the weaker resolution. The optimum value of $\delta y/\delta x$ clearly depends on the local Mach number. For the problems we have examined, values as low as unity have been used to obtain the results presented here.

B. Viscous Flows

1. Laminar Hypersonic Flow Over the Sharp Leading Edge of a Flat Plate

The flow geometry is depicted in panel a) of Fig. 4. The initial sudden deceleration of the flow at the sharp leading edge gives rise to a leading shock which turns the flow away from the wall. Slightly downstream of the leading edge a boundary layer develops turning the flow gradually towards the wall and giving rise to a continuous expansion.

Panel b) of Fig. 4 shows the computed wall pressure distribution for the experimental situation of Bertram.[27] Predictions for a selection of four grid meshes from the many that were tried are shown. The larger number of nodes are distributed in the x-direction in each case; the 100×20 mesh gives results which agree well with the data. The remarks concerning the grid distribution made in Sec. IIIA in connection with inviscid flows also apply here.

Predictions of the surface pressure and heat-transfer distributions are compared with the data of Holden[28] in panels c) and d) of Fig. 4. The data shown are for various freestream Mach and Reynolds numbers. The abscissa quantity was chosen by Holden to correlate all of these data due to scatter; it is not possible to say whether it is entirely successful in so doing. The present predictions were performed using a 100×20 mesh for the indicated two combinations of Mach and Reynolds numbers. The pressure predictions reported by Smith,[29] obtained using a parabolic procedure, are also shown in panel c).

The scatter of the data make a quantitative assessment difficult; the present predictions do, perhaps, overestimate the pressure rise and underestimate the heat transfer. The pressure predictions are certainly superior to those of Ref. 29.

A small dependence on Reynolds number can be discerned in the predictions of panel c).

2. Laminar Shock-Wave/Boundary-Layer Interaction

The flow situation is shown in panel a) of Fig. 5 for the especially interesting case where the incident shock strength is strong enough to cause separation of the boundary layer. Predictions for the experimental interactions studied by Needhan[30] are presented. The Mach number in both cases is 7.4, but the strength of the incident shock is such as to produce an overall pressure rise of 3:1 in the one and 4:1 in the other. The solution domain is indicated on panel a); inflow conditions were not measured so the present predictions were obtained using information at the upstream boundary obtained by a prior calculation of the upstream boundary layer. The predictions were obtained using an 80×25 grid.

Panels b) and c) of Fig. 5 show predictions of the wall-pressure and heat-transfer distributions compared with the data for the less severe impinging shock. Predictions are shown for two values of the boundary-layer thickness at inflow, δ. The smaller value of 0.06 in. is the one determined from the upstream boundary-layer computations. Schlieren photographs of the flow appear to confirm this value. Moreover, the computed upstream profiles agree well with those which emerge from van Driest's[31] similarity analysis so there is no convincing reason to dispute them. Nonetheless, it was found that substantially better agreement with the pressure-distribution data is achieved when δ is increased to the value of 0.09 in. The heat-transfer predictions are, however, adversely affected. We delay further discussion of this until the results for the stronger impinging shock have

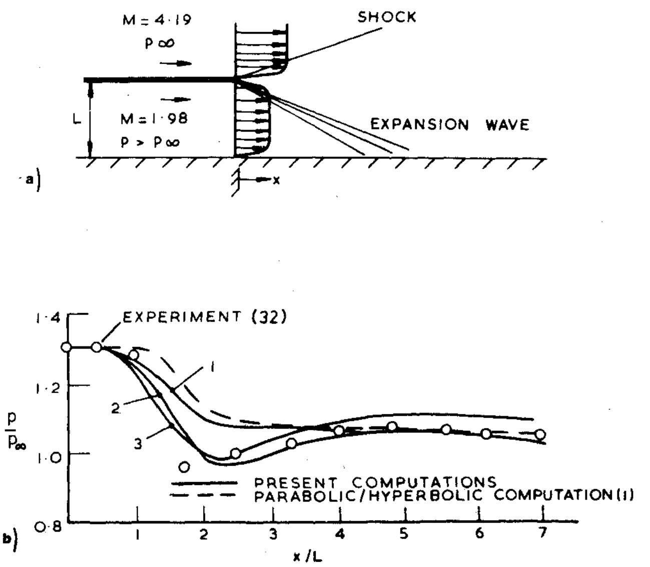

Fig. 7 Turbulent supersonic slot injection: a) flow geometry; b) wall pressure distribution.

been examined. The inviscid solution shown on panel b) demonstrates the major effect of the introduction of viscosity into the computational procedure; it is, of course, in very poor agreement with the data.

Comparisons between the predicted wall-pressure and wall-heat-transfer distributions for the stronger impinging shock of Ref. 30 are shown in panels a) and b) of Fig. 6. The pressure predictions are again improved by augmenting δ, this time to 0.135 in. while the corresponding effect on the heat-transfer predictions is again detrimental.

The influences of artificially thickening the boundary layer may be explained in the following way. The boundary layer is a region of low momentum, the external stream is of high momentum. Within the shock impingement zone, these two regions are separated by a physical discontinuity which is smeared by the computations. In particular, the smeared v-velocities result in the injection of momentum into the boundary layer which tends to suppress separation. Furthermore, the use of the hybrid difference scheme in the y-direction gives a bias in favor of the downward directed mass fluxes when these are larger than the diffusive fluxes. For gird nodes which straddle the shock, significant errors will result. Here also the net effect is the diffusion of momentum into the boundary layer. Increasing the value of δ merely compensates for this defect of the computations. It is interesting to note that a similar problem was encountered by Baldwin and MacCormack[18]; improved predictions were obtained by the introduction of momentum deficit into the freestream.

3. Turbulent Supersonic Slot Injection

Schetz et al.[32] have obtained data for the turbulent supersonic injection of air into a supersonic mainstream; this flow geometry and conditions are illustrated in panel a) of Fig. 7. The authors have attempted, with little success, to predict this experiment using a parabolic/hyperbolic prediction procedure.[1] It is of interest, therefore, to establish the superiority of the elliptic/hyperbolic technique of the present work for this flow.

In the absence of detailed data for the conditions at the slot exit plane, we have assumed a finite value of 2 mm for the thickness of the boundary layer on the bottom wall. The turbulent transport was determined from the rather crude mixing length hypothesis of Prandtl. The computations presented here were obtained using a grid of 80×25 nodes.

Predictions are compared with the data for the wall pressure distribution in panel (b) of Fig. 7. The rather poor parabolic/hyperbolic predictions of Ref. 1 are shown along with three curves obtained using the present method. Curve 1 is obtained when the flow is presumed to be laminar, and when the existence of the boundary layers on the splitter plate is ignored. Curve 2 also assumes laminar flow, but the effect of the splitter plate boundary layers is crudely simulated by introducing a velocity deficit 'spike' into the inflow boundary condition at the splitter plate location corresponding to a Mach number of 0.5. Curve 3 is for turbulent flow with allowance for the splitter plate boundary layers as for curve 2.

Because the parabolic/hyperbolic procedure cannot foresee the upstream propagation of downstream influences within the subsonic layer, the early fall of wall pressure due to the expansion wave is not anticipated by it. The present procedure eliminates this defect. Further, it is evident that the pronounced 'dip' in the pressure distribution, which is its principal feature, is primarily due to the effect of the splitter plate boundary layers rather than to the effects of upstream influence or to the effect of turbulence. The effects of inlet conditions other than the splitter plate boundary layers were found to be insignificant.

IV. Concluding Remarks

1) An existing method for the prediction of steady elliptic flows has been modified to handle near wall supersonic flows.

2) The modified method has been tested against analytical solutions for two-dimensional inviscid flows and, more particularly, against experimental data for two-dimensional, supersonic/viscous, near-wall interactions.

3) More care is required in choosing a satisfactory grid distribution than in the case of purely subsonic calculations. The ratio of cross stream to streamwise grid spacings plays an important role in the supersonic region.

4) The method performs tolerably well and is definitely superior to existing parabolic prediction methods which are unable to simulate the significant elliptic effects which arise due to the existence of the subsonic layer.

5) The inaccuracies in the existing method may be traced to: 1) the effects of the smearing of the pressure waves as a consequence of the failure of the finite-difference formulae to account for the discontinuities of derivatives of variables, and 2) to the hybrid difference scheme which can yield differences that are upwind biased and so contrary to physical reasoning. Further development is required to remove the deficiences.

6) Typical computing times on the CDC 6600 for problems III. B1, III. B2 and III. B3 for the grids stated in the text are: 13 minutes, 17 minutes, and 10 minutes, respectively. These requirements are favorable when compared with those for time-dependent schemes such as in Refs. 14 and 18.

Acknowledgment

The authors wish to acknowledgment the support of the United Kingdom Ministry of Defence for this work under Agreement No. AT/203/109.

References

[1]Issa, R. I. and Lockwood, F. C., "Combined Finite-Difference and Characteristics Procedure for the Prediction of Two-Dimensional Boundary Layers," Internal Rept., Aug. 1975, Mech. Eng. Dept., Imperial College of Science and Technology, London, to appear in *ASME Journal of Fluids Engineering.*

[2]Crocco, L. and Lees, L., "A Mixing Theory for the Interaction Between Dissipative Flows and Nearly Isentropic Streams," *Journal of the Aeronautical Sciences*, Vol. 19, Oct. 1952, pp. 649-676.

[3]Gadd, G. E., "Interactions Between Wholly/Turbulent Boundary Layers and Shock Waves Strong Enough to Cause Separation," *Journal of the Aeronautical Sciences*, Vol. 20, Nov. 1953, pp. 729-739.

[4]Cheng, H. K., Hall, J. G., Golian, T. C., and Hertzberg, A., "Boundary Layer Displacement and Leading Edge Bluntness Effects in High-temperature Hypersonic Flow," *Journal of the Aerospace Sciences*, Vol. 28, May 1961, pp. 353-381.

[5]Stewartson, K., "On the Motion of a Flat Plate at High Speed in a Viscous Compressible Fluid – Part II Steady Motion," *Journal of the Aerospace Sciences*, Vol. 22, May 1955, pp. 303-309.

[6]Lees, L. and Reeves, B. L., "Supersonic Separated and Reattaching Laminar Flows: I – General Theory and Application to Adiabatic Boundary-Layer/Shock Wave Interactions," *AIAA Journal*, Vol. 2, Nov. 1964, pp. 1907-1920.

[7]Brilliant, H. M. and Adamson, Jr., T. C., "Shock Wave/Boundary Layer Interactions in Laminar Transonic Flow," AIAA Paper 73-239, Washington, D. C., 1973.

[8]Reyhner, T. A., and Flugge-Lotz, I., "The Interaction of a Shock Wave with a Laminar Boundary Layer," *International Journal of Non-linear Mechanics*, Vol. 3, June 1968, pp. 173-199.

[9]Flugge-Lotz, I. and Blottner, F. G., "Computation of the Compressible Laminar Boundary-layer Flow Including Displacement Thickness Interaction Using Finite Difference Methods," TR 131, Jan. 1962, Stanford University, California, U. S. A.

[10]Baum, E., "An Interaction Model of a Supersonic Laminar Boundary Layer on Sharp and Rounded Backward Facing Steps," *AIAA Journal*, Vol. 6, March 1968, pp. 440-447.

[11]Ferri, A. and Dash, S., "Viscous Flow at High Mach Numbers with Pressure Gradients," *Proceedings of the Symposium on Viscous Interaction Phenomena in Supersonic and Hypersonic Flow,* Army Research Lab., Wright-Patterson Air Force Base, Ohio, May 1969, pp. 271-317.

[12]Baum, E. and Denison, M. R., "Interacting Supersonic Laminar Wake Calculations by a Finite Difference Method," *AIAA Journal*, Vol. 5, July 1967, pp. 1224-1230.

[13]Garvine, R. W., "Upstream Influence in Viscous Interaction Problems," *The Physics of Fluids*, Vol. 11, July 1968, pp. 1413-1423.

[14]Goodrich, W. D., Lamb, J. P., and Bertin, J. J., "On the Numerical Solution of Two-Dimensional Laminar Compressible Flows with Imbedded Shock Waves," *Trans. ASME, Journal of Basic Engineering*, Vol. 94, Dec. 1972, pp. 765-770.

[15]Butler, T. D., "Numerical Solution of Hypersonic Sharp Leading-edge Flows," *The Physics of Fluids*, Vol. 10, June 1967, pp. 1205-1215.

[16]Tannehill, J.C., Mohling, R.A., and Rakich, J.V., "Numerical Computation of Hypersonic Viscous Flow Over a Sharp Leading Edge," *AIAA Journal*, Vol. 12, Feb. 1974, pp. 129-130.

[17]Cheng, S. I. and Chen, J. H., "A Finite-Difference Solution of Navier-Stokes Equations for Hypersonic Shock Over a Sharp Leading Edge," Third International Conference on Numerical Methods in Fluid Dynamics, Paris, July 1972.

[18]Baldwin, B. S. and MacCormack, R. W., "Numerical Solution of the Interaction of a Strong Shock Wave with a Hypersonic Turbulent Boundary Layer," AIAA Paper 74-558, Palo Alto, Calif., 1974.

[19]Werle, M. J. and Vatsa, V. N., "New Method for Supersonic Boundary-Layer Separation," *AIAA Journal*, Vol. 12, Nov. 1974, pp. 1491-1497.

[20]Patanker, S. V. and Spalding, D. B., "A Calculation Procedure for Heat, Mass and Momentum Transfer in Three-dimensional Parabolic Flows," *International Journal of Heat Mass Transfer*, Vol. 15, Oct. 1972, pp. 1787-1806.

[21]Caretto, L. S., Gosman, A. D., Patankar, S. V., and Spalding, D. B., "Two Numerical Procedures for Three-dimensional Recirculating Flows," *Proceedings of the Third International Conference on Numerical Methods in Fluids Dynamics,* Paris, July 1972.

[22]Runchal, A. K., "Convergence and Accuracy of Three Finite-difference Schemes for a Two-dimensional Conduction and Convection Problem," *International Journal of Numerical Methods in Engineering*, Vol. 4, 1972, pp. 541-550.

[23]Spalding, D. B., "A Novel Finite-difference Formulation for Differential Expressions Involving Both First and Second Derivatives," *International Journal of Numerical Methods in Engineering,* Vol. 4, 1972, pp. 551-559.

[24]Kurkov, A. P., "Mixing of Supersonic Jets Including the Effects of Transverse Pressure Gradient Using Difference Methods," NASA TN-D-6592, Dec. 1971, Lewis Research Center, Cleveland, Ohio.

[25]Liepman, H. W. and Roshko, A., *Elements of Gas Dynamics*, 8th Printing, Wiley, New York, 1967, pp. 100, 296-297.

[26]Issa, R. I., "The Prediction of Supersonic Boundary Layers with Embedded Pressure Waves," Ph.D. thesis, 1974, Imperial College, University of London, London.

[27]Bertram, M. H., "Boundary Layer Displacement Effects in Air at Mach Numbers of 6.8 and 9.6," NACA TN-4133, Feb. 1958, Langley Lab., Va.

[28]Holden, M. S., "Boundary Layer Displacement and Leading Edge Bluntness Effects on Attached and Separated Laminar Boundary Layers in a Compression Corner. Part II: Experimental Study," *AIAA Journal*, Vol. 9, Jan. 1971, pp. 84-93.

[29]Smith, F., "The Numerical Solution of Hypersonic Laminar Boundary Layer Problems," Ph.D. thesis, 1973, Imperial College, University of London, London.

[30]Needham, D. A., "Laminar Separation in Hypersonic Flow," Ph.D. thesis, 1965, Imperial College, University of London, London.

[31]Van Driest, E. R., "Investigation of Laminar Boundary Layer in Compressible Fluids Using the Crocco Method," NACA TN-2597, Jan. 1952, North American Aviation Inc., Downey, Calif., U.S.A.

[32]Schetz, J. A., Gilreath, H. E., Waltrup, P. J. and Lewis, D. P., "Research on Slot injection into a Supersonic Air Stream," Maryland University, College Park, Md., AERO-68-1, Sept. 1968.